IOPscience iopscience.iop.org

Home Search Collections Journals About Contact us My IOPscience

A new critical point in the non-linear conductivity due to variable-range hopping in Si

This article has been downloaded from IOPscience. Please scroll down to see the full text article.

1997 J. Phys.: Condens. Matter 9 881

(http://iopscience.iop.org/0953-8984/9/4/008)

View the table of contents for this issue, or go to the journal homepage for more

Download details:
IP Address: 171.66.16.207
The article was downloaded on 14/05/2010 at 06:13

Please note that terms and conditions apply.

J. Phys.: Condens. Matter **9** (1997) 881–888. Printed in the UK PII: S0953-8984(97)78269-9

A new critical point in the non-linear conductivity due to variable-range hopping in Si

P Stefanyi†, C C Zammit†, P Fozooni†, M J Lea† and G Ensell‡

† Department of Physics, Royal Holloway, University of London, Egham, Surrey TW20 0EX, UK

‡ Department of Electronics and Computer Science, University of Southampton, Southampton SO17 1BJ, UK

Received 1 October 1996, in final form 29 October 1996

Abstract. A new critical point and a non-equilibrium phase transition in the non-linear conductivity in doped silicon have been observed in the variable-range hopping regime, due to a negative differential resistance with a dc bias current I_{dc}. We show this critical behaviour is intrinsic in a thermal model, and for a resistance–temperature characteristic given by the Efros–Shklovskii law $R(T) = R_0 \exp(T_0/T)^{1/2}$ we find a critical temperature $T_c = 0.005\,12T_0$, independent of R_0 and the electron–phonon coupling strength. Below T_c this gives circuit-limited oscillations with a frequency $f \propto I_{dc}$.

Variable-range-hopping (VRH) in doped semiconductors is of considerable scientific interest [1] and of technological importance, particularly in cryogenic particle detectors [2]. In the elemental semiconductors Si and Ge, as in other materials, the resistance–temperature characteristic in the hopping regime at low temperatures is given by

$$R(T) = R_0 \exp(T_0/T)^m \tag{1}$$

where $m = 1/4$ for Mott hopping or $m = 1/2$ for Efros–Shklovskii hopping with a parabolic Coulomb gap (a 'soft gap') in the impurity band at the Fermi level. In many cases, $m = 1/2$ is a good approximation experimentally, though deviations from $m = 1/2$ have been observed in both n- and p-type Si below 100 mK [3]. Two explanations have been put forward: that a 'hard gap' opens up in the density of states below 100 mK which gives activated conduction, or that there is a temperature dependent smearing of the Coulomb gap and the true Coulomb gap is only seen at very low temperatures. VRH thermometric sensors are used for the detection of x-rays [4] or for exotic dark-matter particles [2], with the sensors attached to a suitable target. The measurements presented here were made as part of the development of a cryogenic particle detector [5]. A dc bias current is passed through the semiconductor and the transient temperature rise is measured when a particle is absorbed in the target. The bias current itself can produce significant heating and a reduction in resistance to $R(T_e)$, described by an effective temperature $T_e > T_{ph}$, the phonon temperature in the sensor. A thermal model was developed by Wang *et al* [6] in which the Joule heating $\dot{Q} = I_{dc}^2 R(T_e)$ flows from the electrons to the phonons via electron–phonon coupling given by

$$\dot{Q} = A\left(T_e^\alpha - T_{ph}^\alpha\right) \tag{2}$$

0953-8984/97/040881+08$19.50 © 1997 IOP Publishing Ltd

where the exponent α may vary from five to eight, depending on the material and the sample. A simple interpretation is that T_e is an effective electron temperature, though this is perhaps inconsistent with the conventional picture of phonon-assisted hopping. Alternatively, (2) may be regarded as a parametrization of the dependence of R on the input power. There is no doubt that it gives a very good account of the effects of a bias current in many VRH samples [7, 8], including those studied here. The phonons then transfer the heat to the heat sink. An optimum bias current must be chosen to maximize the detector sensitivity.

An analysis of (1) and (2) leads to a simple and remarkable result, which is intrinsic to hopping or activated conduction when these equations apply. As the input power raises the effective temperature T_e, the resistance $R(T_e)$ falls, giving non-linear effects, as the voltage across the sample $V = IR(T_e)$ may then decrease with increasing current. The turning points $\mathrm{d}V/\mathrm{d}I = 0$ occur for electron temperatures which are given by the solutions of

$$(\alpha/m)\left(T_e/T_0\right)^m = 1 - \left(T/T_e\right)^\alpha \tag{3}$$

where $T_e \geqslant T$, the phonon temperature T_{ph} or the base temperature T_B if the phonon–phonon resistance is small. For instance, with $m = 1/2$ and $\alpha = 5$, then for $T > T_c = 0.005\,12T_0$ there are no solutions to (3) and V is a monotonically increasing function of I. But for $T < T_c$ there are two solutions and the I–V characteristic has a distinctive 'S-shape' with a negative-differential-resistance (NDR) region. Surprisingly, (3) shows that the critical temperature T_c should be independent of both R_0 and the strength A of the electron–phonon coupling. It depends only on the temperature dependence of the resistance and the coupling. The values of the critical temperature T_c/T_0 are given in table 1 for several values of α and the values of m corresponding to Mott, Efros–Shklovskii and nearest-neighbour hopping. Both α and m can be accurately determined experimentally. Associated with the critical temperature, which is independent of the sample geometry, is a critical current I_c and a critical voltage V_c (or a critical electric field E_c). For a current source an NDR region leads to instabilities, oscillations and non-equilibrium phase transitions as studied in other semiconductors [9] such as p-type Ge [10, 11], δ-doped GaAs [12] and heterostructure superlattices [13] where non-linearity can result from avalanche breakdown and other mechanisms. An important feature of this new critical point is that it is intrinsic to the conduction mechanism and related to a well defined physical parameter T_0.

Table 1. Critical temperatures T_c/T_0 for non-linear hopping conduction.

	$m = 1/4$	$m = 1/2$	$m = 1$
$\alpha = 4$	5.89×10^{-6}	7.13×10^{-3}	0.134
$\alpha = 5$	2.80×10^{-6}	5.12×10^{-3}	0.117
$\alpha = 6$	1.50×10^{-6}	3.86×10^{-3}	0.103
$\alpha = 7$	0.87×10^{-6}	3.02×10^{-3}	0.093

Measurements of this non-linear critical temperature and the associated non-equilibrium phase transition were made in epitaxial Si:As grown by chemical vapour deposition (CVD) with a thickness of 8.4 μm $\pm$ 5% and a dopant concentration of 7.36×10^{18} cm^{-3}. The samples consisted of two separate sensors on the same Si substrate, with ion-implanted ohmic contacts, each 1.2 mm $\times$ 3.0 mm in area. The double sensor was glued to a large rectangular Si block as a heat sink at the base temperature T_B. Superconducting Al wires, 25 μm in diameter, gave electrical contact while maintaining thermal isolation.

The temperature dependence of the resistance $R(T)$ was measured using a low-power ac bridge, model AVS-46, or using dc techniques with a Keithley 236 current source and

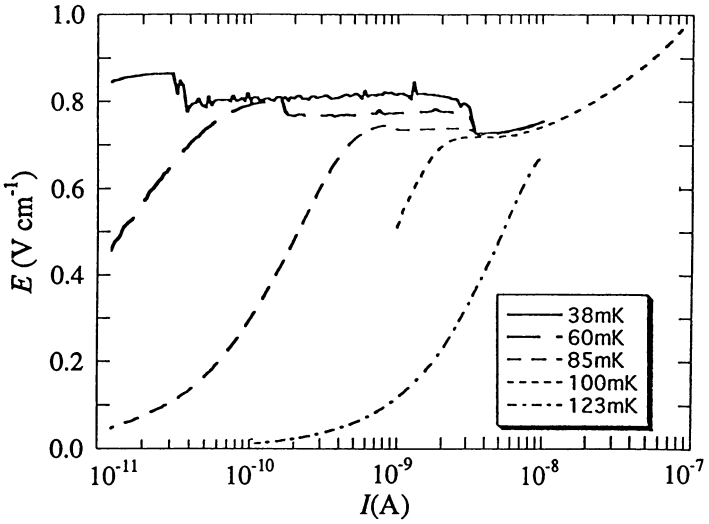

Figure 1. The electric field E versus the current I, in an Si sensor, measured with a dc current source at $T = 38$, 60, 85, 100 and 123 mK.

voltmeter. A typical pair of sensors had $m = 1/2$ with $R_0 = 25.4\ \Omega$, $T_0 = 22.5$ K and $R_0 = 22.0\ \Omega$, $T_0 = 26.9$ K above 120 mK, in agreement with (1). The double-sensor arrangement enabled the temperature-dependent electron–phonon coupling and the phonon–phonon coupling to the heat sink to be measured separately using one sensor to monitor the phonon temperature T_{ph} (measured at low power) while higher power was supplied to the other sensor whose resistance was used to determine the effective temperature T_e from (1). Above 100 mK the electron–phonon coupling was given by (2) with $\alpha = 5.04 \pm 0.1$ and with $A = 0.8 \times 10^{-4}$ W K^{-5} for a typical sensor. The phonon–phonon coupling between the phonons in the sensors and the heat sink at T_B was given by $\dot{Q} = B(T_{ph}^{3.5} - T_B^{3.5})$ with $B = 0.8 \times 10^{-4}$ W K$^{-3.5}$. Almost identical exponents were found in ion-implanted Si:As by van der Heijden *et al* [8].

The V–I characteristics were measured directly using dc currents at low powers or with pulsed currents (pulse duration 20 ms). Typical characteristics at currents below 10^{-7} A are shown in figure 1 where the electric field E across the sensor is plotted versus the dc excitation current I_{dc} at 38, 60, 85, 100 and 123 mK (note the linear–log scale). Linear behaviour was observed below 200 mK only for $E < 0.5$ V cm^{-1}. At higher electric fields strong non-linear behaviour was found, which can be characterized as breakdown. Below l00 mK there was a region of currents where the field was almost constant at about 0.75 V cm^{-1} [14]. The range of currents with this peculiar behaviour extended to lower currents as the temperature decreased. This is a region of NDR, $\mathrm{d}V/\mathrm{d}I < 0$, with instabilities, oscillations and switching as a consequence. At higher currents, above 5 nA, the measured E–I curves were almost temperature independent for base temperatures below 125 mK with $\mathrm{d}V/\mathrm{d}I > 0$.

The Si sensors also exhibited spontaneous oscillations in the range of the NDR of the E–I curves. Figures 2(*a*) and (*b*) show the dependence of the amplitude and frequency respectively of these oscillations on the bias current for various temperatures, measured via a low-noise Coshise preamplifier. At l00 mK, the oscillations started spontaneously

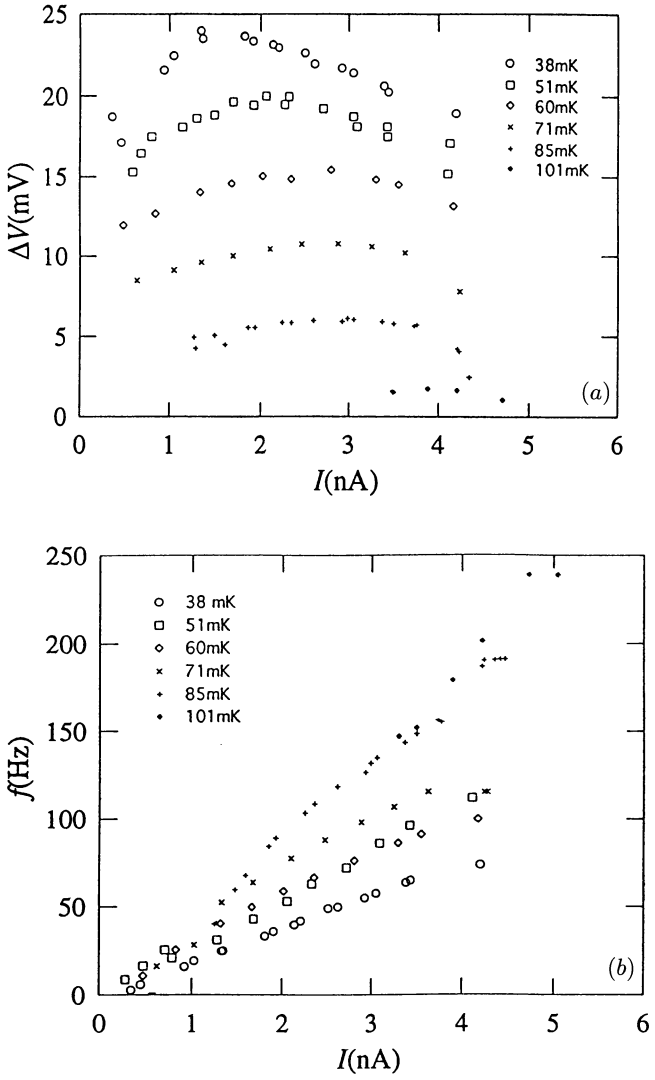

Figure 2. (*a*) The amplitude ΔV and (*b*) the frequency f of the spontaneous oscillations versus the bias current at $T = 38$, 51, 60, 71, 85 and 101 mK.

at ∼3 nA bias current at the point of minimum differential resistance on the *E–I* curve in figure 1. With increasing bias current the oscillations rapidly became periodic with an increasing fundamental frequency, below 250 Hz, with almost constant amplitude. At 5 nA the oscillations became chaotic with smaller amplitude and indistinguishable frequency and disappeared at higher currents. At lower temperatures the region of bias currents with spontaneous oscillations widened, approximately corresponding to the constant-electric-field regions in figure 1, and the amplitude increased. The frequency of the oscillations was proportional to the bias current with a slope which decreased with decreasing temperature.

These oscillations are similar to those seen in thermally activated germanium near 6.2 K as described by Lehr *et al* [10] and by Rau *et al* [11] where strong non-linearities arise

from impurity impact ionization, which leads to filamentary current flow in low-resistance channels [15]. Rau *et al* [11] classified the oscillations into two types: *circuit-limited oscillations* (CLO) and *structure-limited oscillations* (SLO). The CLO type occurred at low bias currents and were modelled as the charging and discharging of the circuit capacitance through the sensor, which switches from a high resistance R_1 to a low resistance R_2 at a certain threshold voltage V_t. The capacitance C then discharges through R_2 until the sensor switches back to R_1 at a lower voltage V_h. This system can then oscillate with a frequency f given by

$$I_{dc} = \Delta Q\, f = \Delta V\, Cf \tag{4}$$

where ΔQ is the charge which passes through the sensor in each oscillation and $\Delta V = V_t - V_h$ is the amplitude of the oscillations. All the features expressed in (4) are clearly seen in our data. First, figure 2(*a*) shows that the amplitude ΔV of the oscillations is almost independent of bias current, as expected, since ΔV is the difference in the switching voltages. Consequently, (4) predicts that $f \propto I_{dc}$ as shown in figure 2(*b*). The values correspond to a circuit capacitance $C \sim 2$ nF. The frequency decreased as expected with the addition of an external capacitance. In the Si sensors the region of SLO is not so well resolved but is certainly present on the side of high bias currents where the oscillations disappear, with the characteristics of decreasing amplitude and chaotic behaviour [9–11].

This oscillatory behaviour exhibits the features of a nonequilibrium phase transition [9]. The amplitude of the oscillations decreased with increasing temperature and disappeared above a critical temperature T_c. The conditions for the onset of oscillations at T_c define a critical current I_c and a critical voltage V_c. By introducing $\Psi = I - I_c$ as an order parameter and $F = V - V_c$ as an ordering field respectively, Lehr *et al* [10] used the Landau theory for phase transitions to show that the V–I characteristic at a temperature T can be written as

$$V = V_0 + a\big(I - I_0\big) + b\big(I - I_0\big)^3 \qquad a = a_0\big(T - T_c\big) \qquad a_0 > 0 \qquad b > 0. \tag{5}$$

At the critical temperature $V_0 = V_c$ and $I_0 = I_c$; in general these parameters will be temperature dependent. For $T > T_c$ the V–I curves are monotonic and the semiconductor has a continuous transition from high to low resistance as I increases. Below the critical temperature, the V–I curves enter an NDR region, with the spatio-temporal coexistence of high- and low-resistance states or phases, as shown in figure 3 where the critical point is marked as C. The dashed line shows the locus of the extremal points, $\mathrm{d}V/\mathrm{d}I = 0$ for different temperatures. As I increases, the electric field reaches the lower extremal point and the sensor then oscillates between high- and low-resistance states. The locus of the oscillations on the E–I plot is shown by the horizontal lines for $T = 85$ mK. The oscillations continue until the dc current increases above the upper extremal point, which always lies close to the critical point C. Above this region the characteristics are almost independent of the base temperature. Below T_c the voltage difference between extremal points is $\Delta V = 4\{a_0(T_c - T)/3\}^{3/2} b^{-1/2} = V_t - V_h$. Hence we can plot $\Delta V^{2/3}$ versus T as shown in figure 4, which gives a good straight line. Extrapolating the line to zero amplitude gives a critical temperature $T_c = 115$ mK. The critical voltage $V_c = 88$ mV and the critical current $I_c = 3$ nA. This critical temperature is close to the theoretical value $T_c \cong 0.005\,12 T_0 = 115 \pm 4$ mK, and strongly supports our interpretation.

We modelled the I–V curves in detail, assuming that the sensor and the current density were homogeneous and that all the Joule heat produced in one sensor went into the phonon system in the double sensors and substrate and from there to the heat sink through the glued interface. We parametrized this model [6] using the $R(T)$ characteristics (1) and the

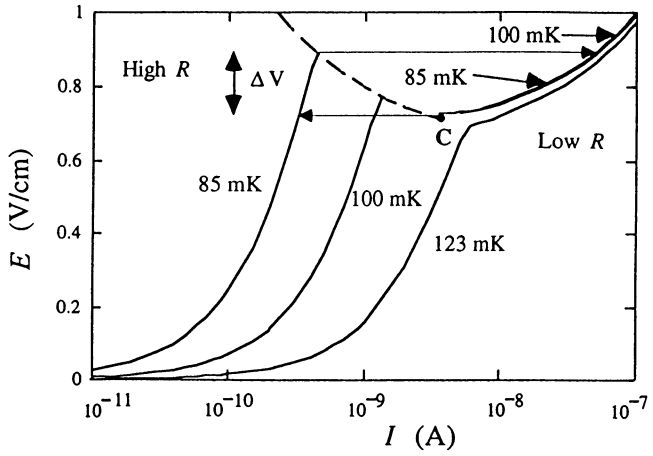

Figure 3. The E–I characteristics and phase diagram for the non-linear electronic transport in a semiconductor, from model calculations with a critical temperature of 115 mK. The critical point is marked as C. The characteristics are shown for $T < T_c$ at 85 and 100 mK, and for $T > T_c$ at 123 mK. The horizontal lines show the paths followed during the oscillations.

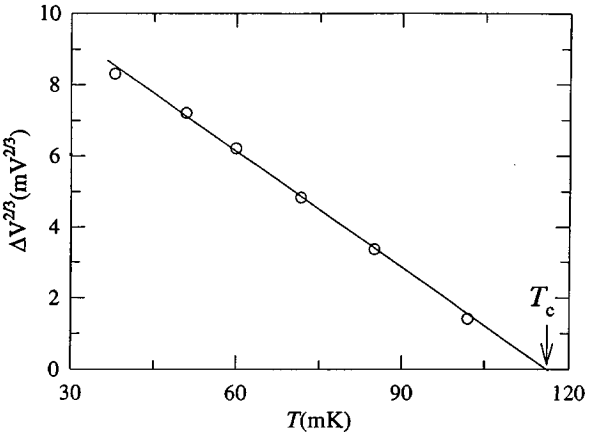

Figure 4. The amplitude of the oscillations $\Delta V^{2/3}$ versus the temperature T, showing T_c at 115 mK.

measured heat flux (2) where $\dot{Q} = IV$ is the Joule heating. But the homogeneous model gives high values of the critical current $I_c = 26$ nA, well above the experimental value.

However, the hopping process is intrinsically inhomogeneous at the microscopic level with the current following the percolation paths with the lowest resistances. Hence thermal breakdown would initially be very localized and could start with a filament of high current density in a very similar way to that postulated in Ge at higher temperatures [10, 11]. To model this we considered an individual sensor as two parallel resistors: a filament with a fraction β of the volume and a resistance $R_1 = R(T)/\beta$, and the rest with a fractional volume $(1 - \beta)$ and a resistance $R_2 = R(T)/(1 - \beta)$, with a total current $I = I_1 + I_2$. We then assume that the Joule heat transfer (given by (2) but proportional to the volume) from

the electrons in the filament to the phonons is a factor of γ worse than for the rest of the sensor, and that the electron temperatures, T_1 and T_2, in the two parts are decoupled. We immediately find that for $\beta < 0.1$ and $\gamma < 0.2$ the 'filament' can be significantly warmer (higher effective temperature) than the rest of the sensor. For a wide range of values of β and γ, NDR is observed with a critical temperature $T_c = 115$ mK. The model critical temperature is the same as for a homogeneous sample, as $T_c = 0.005\,12T_0$ is independent of the strength of the electron–phonon coupling and hence also applies to inhomogeneous samples with the same $R(T)/R_0$ temperature dependence. Choosing values of $\beta = 0.02$ and $\gamma = 0.18$, the E–I characteristics are plotted in figure 3 at 85, 100 and 123 mK for currents up to 10^{-7} A. The critical behaviour is clearly seen and, for these parameters, we find $T_c = 115$ mK, $V_c = 81$ mV and $I_c = 3.1$ nA, in good agreement with the experimental values of 115 mK, 88 mV and 3 nA respectively. It seems quite probable that a distribution of resistivities and the electron–phonon coupling will be found even in CVD-grown semiconductors and that local 'hot spots' will occur.

This thermal model was the simplest which gave a good account of the E–I curves (actually to very high current values greater than 1 mA, well above the critical region). The general features were relatively insensitive to the precise values of β and γ. Other combinations of parameters, and of parallel and series resistors, could have been used. The value of $\beta = 0.02$ corresponds to a filament width of 25 μm, comparable with the thickness (8.4 μm) of the CVD layer. The free edges of the sensor area were defined by cleaving the silicon substrate wafer to minimize the damage. This might decrease γ at the edges and trigger the thermal breakdown and reduce the critical current but would not change the basic phenomenon or the critical temperature T_c. Even in homogeneously doped Si the effects should occur.

Another source of non-linearity in the VRH region is the effect of the applied electric field E on the VRH resistivity (the electric field model), as found in ion-implanted Si and in Ge [16]. In general $R(E, T) = R(0, T)G(E, T)$, where G is some exponential function. Zhang *et al* [7] and van der Heijden *et al* [8] showed that, for sample parameters (principally T_0) in ion-implanted Si similar to those in the present experiments, the thermal model gave a better fit to the data than the electric field model. This is confirmed by the excellent fit to (2) which we find for the temperature-dependent electron–phonon coupling. Also for the electric field model the current for a given field is $I \propto E/G(E, T)$ which does not exhibit any critical behaviour and would lead to E–I plots which would depend on the base temperature even at high currents, in contrast to the observations and the model used here. It seems that the electric field effects are relatively small in these experiments.

We conclude that there is an intrinsic breakdown region in the VRH regime for doped semiconductors below a critical temperature T_c which is proportional to T_0. This leads to instabilities and, in particular, CLO at a frequency $f \propto I_{dc}$. The values of the critical current in these epitaxial silicon samples can be explained by filamentary thermal breakdown at local 'hot spots' in the sample due to spatial variations in the electron–phonon coupling.

Acknowledgment

We would like to thank Dr R W van der Heijden for useful discussions, the staff of the Silicon Microfabrication Facility at Southampton University for sample preparation, the technical staff at Royal Holloway for assistance with the experiments, other members of the UK Dark Matter Programme and the SERC (PPARC) for a research grant.

References

[1] Shklovskii B I and Efros A L 1984 *Electronic Properties of Doped Semiconductors* (Berlin: Springer)

[2] Sadoulet B 1993 *J. Low Temp. Phys.* **93** 821; see *J. Low Temp. Phys.* **93** for *Proc. 5th Int. Workshop on Low Temperature Detectors*

[3] van der Heijden R W, Chen G, de Waele A I A M, Gijsman H M and Tielen F P B 1991 *Solid State Commun.* **78** 5
Dai P, Zhang J and Sarachik M P 1992 *Phys. Rev. Lett.* **69** 1804
Zhang J, Cui W, Juda M, McCammon D, Kelley R, Moseley S H, Stahle C K and Szymkowiak A E 1993 *Phys. Rev.* B **48** 2312
Shlimak I S, Kaveh M, Ussyshkin R, Ginodman V, Baranonovski S D, Thomas P, Vaupel H and van der Heijden R W 1995 *Phys. Rev. Lett.* **75** 4764

[4] Zammit C C, Sumner T J, Hepburn I D and Ade P A R 1991 *Nucl. Instrum. Methods* A **310** 244
Kelley R L, Moseley S H, Stahle C K, Szymkowiak A E, Juda M, McCammon D and Zhang J 1993 *J. Low Temp. Phys.* **93** 287

[5] Stefanyi P, Zammit C C, Rentzsch R, Fozooni P, Saunders J and Lea M J 1994 *Physica* B **194–196** 9

[6] Wang N, Wellstood F C, Sadoulet B, Haller E E and Beeman J 1990 *Phys. Rev.* B **41** 3761

[7] Zhang J, Cui W, Juda M, McCammon D, Plucinsky P P, Sanders W T, Snedeker C, Kelley R, Holt S S, Madejski G M, Moseley S H and Szymkowiak A E 1991 Unpublished notes from the *Workshop on Semiconductor Thermistors for Millikelvin Operation (Berkeley, CA, 1991)*

[8] van der Heijden R W, Chen G, de Waele A T A M, Gijsman H M and Tielen F P B 1992 *Phil. Mag.* B **65** 849

[9] Schöll E 1987 *Nonequilibrium Phase Transitions in Semiconductors* (Berlin: Springer)

[10] Lehr M, Huebener R P, Rau U, Parisi J, Clauss W, Peinke J and Roehricht B 1990 *Phys. Rev.* B **42** 9019

[11] Rau U, Clauss W, Kittel A, Lehr M, Bayerbach M, Parisi J, Peinke J and Huebener R P 1991 *Phys. Rev.* B **43** 2255

[12] Kehner B, Quade W and Schöll E 1995 *Phys. Rev.* B **51** 7225 and references therein

[13] Wacker A, Schwarz G, Prengell F, Schöll E, Kastrup J and Grahn H T 1995 *Phys. Rev.* B **52** 13 788 and references therein

[14] A similar feature can be seen in figure 1 of [8] in an ion-implanted Si:As sensor at 78 mK.

[15] Peinke J, Richter R and Parisi J 1993 *Phys. Rev.* B **47** 115
Hüpper G, Pyragas K and Schöll E 1993 *Phys. Rev.* B **47** 15 515

[16] Grannan S M, Lange A E, Haller E E and Beeman J W 1992 *Phys. Rev.* B **45** 4516